IEEE Access
Multidisciplinary | Rapid Review | Open Access Journal

Received December 23, 2019, accepted February 3, 2020, date of publication February 19, 2020,
date of current version February 28, 2020.

Digital Object Identifier 10.1109/ACCESS.2020.2975052

Radar Simulation of Wake Vortices in Rainy Conditions Based on the Euler-Euler Multiphase Model

ZHOU JIN-XIN[1], LI DONG[1,2], AND ZHANG ZE-YU[1]
[1]School of Aeronautics, Northwestern Polytechnical University, Xi'an 710072, China
[2]National Key Laboratory of Aerofoil/Foil Grid Aerodynamics, Northwestern Polytechnical University, Xi'an 710072, China

Corresponding author: Li Dong (ldgh@nwpu.edu.cn)

This work was supported in part by the National Natural Science Foundation of China under Grant U1733203.

ABSTRACT The radar monitor of aircraft wake vortex is of great significance to air traffic control. Comparing with the case in clear air, the radar signal of wake vortices in rainy conditions is more easily captured due to the higher levels of signal. To able to analyze radar echo characteristics of evolving wake vortices, the numerical simulation of the evolution of the wake vortices in various rain rates has been performed based on the Euler-Euler frame. The result shows that the rainfall can accelerate the decay of wake vortices. A radar simulator has been represented to process the radar echo signal of raindrops around the wake vortex. The Doppler spectrum of echo signals in radar resolution volumes has been analyzed and the straight vortex and the vortex ring phases show different characteristics of spectrum width. The Doppler width information based on this result of interaction between the wake vortex and rain can be used for assessing the decay phase of wake vortices and monitoring potential hazard for wake vortex encounters.

INDEX TERMS Eular-Eular model, rain rate, radar simulator, aircraft wake vortices.

I. INTRODUCTION

Aircraft wake vortex is a by-product of the lift, which is a pair of counter-rotating vortices. It will have a considerable influence on the flight attitude of the following aircraft, causing it to roll motion or altitude loss for wake encounter aircrafts, which is fatal in the take-off and landing phase. However, with the vigorous development of commercial aviation and the rapid increase in airport traffic, the take-off and landing efficiency of aircraft is becoming increasingly important, which is related to the throughput and economic benefits of the airport and has become a key factor restricting the capacity of air transport. In order to balance efficiency and safety, the wake separation standard has been formulated to limit airport capacity in civil aviation management, e.g. ICAO and REACT-EU standard. The formulation of these standards depends on the deep understanding of the wake vortices. At present, the research methods of wake vortices mainly include computational fluid dynamics and experimental measurements.

CFD is a useful tool for investigating wake vortices behavior and its advantage is that it is very convenient to take various ambient conditions into account, for example, turbulence, ground and wind. In addition, CFD results can present each stage of wake vortex evolution and it's very helpful for us to understand roll-up and dissipation mechanism of that under different environments. This makes up for the shortcomings of wind tunnel measurements since, for almost all wind tunnel measurements, only the near and extended near field (down to the order of 10 wing spans) can be measured due to the length limitation of wind tunnel test section. Validated CFD simulation can predict the wake vortex characteristics from the near field to far-field. For the air traffic manager, the field measurement is a more direct and effective approach for wake vortices monitoring and detection which mainly include radar and lidar since the measurement is implemented in the airport along the path of approach and take-off. Lidar can identify the position of the wake vortex and calculate the velocity distribution through data processing and however lidar works well only in clear air. Under foggy and rainy weather, radar has better performance for identifying wake vortices. The trails on Paris Orly airport have proved that the usability of X-band Doppler Radar in different weather conditions like fog, rain and dry/wet air [1]. As dragged by wake vortices, raindrops will be rolled up and have various velocities in magnitude and direction.

The associate editor coordinating the review of this manuscript and approving it for publication was Rosario Pecora.

For raindrops or fog droplets, there is increased clustering in regions of lower vorticity and higher strain rates [2] and therefore raindrops around wake vortices are strong scatterers and can generate higher-level radar echo signals. Doppler spectrum produced by signal processing can reflect the velocity characteristics of raindrops [3]. Then the information of wake vortices including intensity and position can be retrieved through Doppler shift frequencies. In order to produce scenarios of interest conveniently and optimize radar processing technology, weather radar-like signals are simulated to provide a deterministic and controlled environment for signal processing. Capsoni *et al.* [4] represented a physically based software radar simulator that properly takes the characteristics of the radar system, the effects of propagation and wave polarization into account and indicated the radar signal is the summing of all the contributions coming from each scatterer. Cheong *et al.* [5] proposed a radar simulation method based on table lookup and linear interpolation to simulate radar signals for studying many types of atmospheric conditions. Then a three-dimensional radar simulator was designed which is able to generate simulated raw time series data, and the radar signals are derived from a high-resolution numerical weather model [6]. Liu *et al.* [7], [8] used a radar simulator to model the radar signature of raindrops within wake vortices and proposed that the Doppler signature is a potential criterion for identifying wake vortex hazards. Jeannin *et al.* [9] further developed the radar signature simulation frame in rainy weather and emphasized the computation of the raindrop concentration in the wake vortex region. Li *et al.* [10] well estimated velocities and accelerations of the raindrops around wake vortices, proposed a circulation retrieval method based on a vertically pointing radar under the rain condition and verified the retrieval method through numerical simulation results. In these studies, however, wake vortices were treated as static velocity fields and did not evolve with time. This leads to the motion of raindrops caused by this oversimplified wake vortex field be far away from reality. In order to make simulated radar signals of raindrops reflect the characteristics of wake vortices accurately, a more realistic rain flow field within wake vortices is needed.

In this paper, the wake vortex is generated by a medium type aircraft A320, which defined by ICAO. the Euler-Euler multiphase model is represented to simulate the wake vortex evolution in rainy conditions. The interaction between wake vortices and rain is considered and this makes the dynamics of the raindrops closer to reality. The radar signal of raindrops within wake vortices is generated by a radar simulator. The Doppler spectrum under various evolution phases of wake vortex is analyzed. The details of these models and methods are described below.

II. GOVERNING EQUATIONS BASED ON THE EULER- EULER MULTIPHASE MODEL

In the Euler-Euler approach, each phase is treated as a continuous medium and these phases are assumed to interpenetrating which leads to phasic volume fractions being introduced into governing equations. For each phase, the momentum and continuity equation are needed to solve. The coupling of different phases is achieved through interphase exchange coefficients. For the simulation of the wake vortex field, the Boussinesq-approximated Navier-Stokes equations with a source term that represents the interphase force are solved and a Lagrangian dynamic Smagorinsky model is applied. The governing equations in partial differentia form are as follows:

$$\frac{\partial u_j}{\partial x_j} = 0 \tag{1}$$

$$\rho\frac{\partial u_i}{\partial t} + \rho u_j\frac{\partial u_i}{\partial x_j} = -\frac{\partial p}{\partial x_i} + \mu\frac{\partial}{\partial x_j}\left(\frac{\partial u_i}{\partial x_j}\right) - \frac{\partial \tau_{ij}}{\partial x_j} + S \tag{2}$$

where u_i is the component of velocity of wake vortex field, ρ is air density, μ is air vorticity, τ_{ij} is the subgrid-scale stress and S is the interaction force between phases given by [11]

$$S = \rho_w a\frac{18\mu C_D \mathrm{Re}}{24\rho_w D^2}(u - u_w) \tag{3}$$

where C_D is the drag coefficient, Re is the relative Reynolds number, D is the diameter of the raindrop, ρ_w is the density of water a_k is the volume fraction of rain phase and $(u - u_w)$ is the velocity difference between rain phase and air phase. The variable of the volume fraction does not appear in the continuity equation or transient and convective term of the momentum equation (that is, the volume fraction is specified as 1) since the contribution of the volume fraction to the velocity field is much less than that of the interphase force.

For the rain phase, continuity and momentum equation are defined as follows:

$$\frac{\partial a\rho_r}{\partial t} + \frac{\partial(a\rho_r u_{rj})}{\partial x_j} = 0 \tag{4}$$

$$\frac{\partial a\rho_r u_{ri}}{\partial t} + \frac{\partial(a\rho_r u_{ri}u_{rj})}{\partial x_j} = a\rho_r g_i + S \tag{5}$$

where $a\rho_r$ can be considered as the effective density and g_i is the gravity acceleration. In equation (5), in addition to the drag force between the phases, the effect of the gravity of raindrops and on raindrop motion is also considered. This Eulerian multiphase model has been validated in the wind-driven rain simulation [11].

III. INITIAL AND BOUNDARY CONDITION

The wake vortices were initialized as the superposition of two B-H vortices, which comprises the following equation for the tangential velocity v as a function of the initial circulation Γ_0, the vortex core radial r_c and the distance from the core r,

$$v_\theta = \frac{\Gamma_0}{2\pi}\frac{r}{r^2 + r_c^2} \tag{6}$$

The initial circulation Γ_0 generated by A320 is 200 m^2/s, the vortex space $b_0 = 26.6$ m and the vortex core radial r_c is 1.5 m. The initial descent velocity $w_0 = \Gamma_0/(2\pi b_0) = 1.2$ m/s and hence the time scale $t_0 = b_0/w_0 = 22.2$ s. The initial tangential velocity of the vortex pair is shown

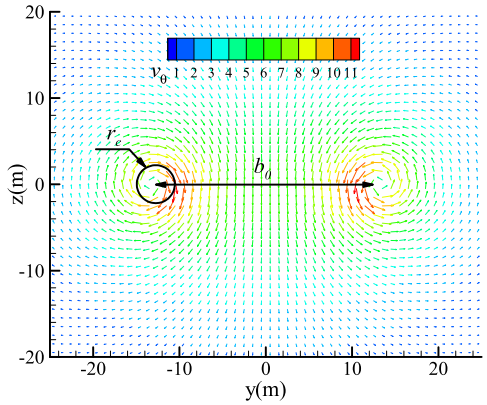

FIGURE 1. Tangential velocity of the wake vortex flow field generated by B-H model.

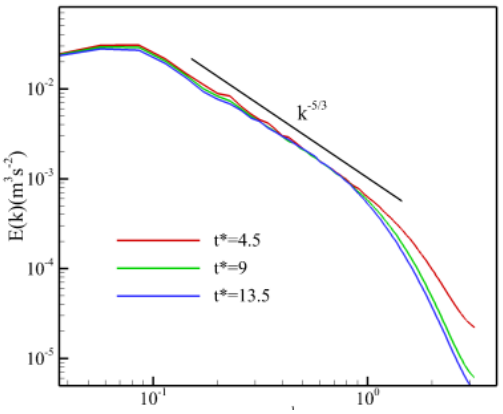

FIGURE 2. Energy spectrum of the initial turbulent flow field with $\varepsilon^* = 0.05$.

in Figure 1. Then the wake vortex field is superimposed on a pre-generated ambient turbulent field with moderate intensity ($\varepsilon^* = (\varepsilon b_0)^{1/3}/w_0 = 0.05$, where ε is the dissipate rate of turbulence.). The initial turbulent field is generated using Rogallo method [12], which obeys a modified von Karman spectrum [13]. Before the vortex field is superimposed, a pre-run of LES of the turbulent flow field is performed until the eddy dissipation ratio reaches stability as shown in Figure 2.

In this simulation, three moderate to low rain rates (the initial volume fraction of rain flow field) are considered: 0mm/h, 5mm/h and 10mm/h, respectively. The chosen size of the computational domain is $L_x \times L_y \times L_z = 8.5\, b_0 \times 8.3\, b_0 \times 12.4 b_0$ with a uniform grid resolution of $\Delta = 1$m (total gird points $226 \times 220 \times 330$), where x, y and z correspond the flight, vertical and span direction, respectively. The domain size in the flight, 8.8 b_0, is lager enough to simulate the impact of Crow instability on the decay of the wake vortex system. For the wake vortex flow field, all boundaries of the computational domain are periodic. The top and bottom boundaries of the rain flow field are Dirichlet and Neumann conditions, respectively. The numerical time step is fixed as 0.01 s.

IV. RADAR SIMULATOR

In the presence of wake vortices, the trajectory and the concentration of raindrops will be affected by the position and circulation of vortices. Therefore, the radar response from raindrops could be used to retrieve the main characteristics of wake vortices. To analyze the radar scattering characteristics of raindrops around wake vortices, a radar simulator is used to compute the radar signature.

A. BASIC STRUCTURE OF THE RADAR SIMULATOR

The radar echo is a composite signal which depends on the velocity and reflectivity of scatterers. In a radar resolution volume, the signal received from transmitted pulses is regarded as to the summing of returned echoes from all discrete scatterers. In the simulation of this paper, the rain phase is regarded as a continuous medium because there is no discrete point in the calculation domain because of the Euler multiphase model. To solve this problem, a certain amount of scatterers, namely raindrops, is positioned within the rain phase flow field and the velocity of each raindrop is interpolated based on different positions in space. For a sample point on time series, the received signal is a complex sum of the Doppler shift signal from all the individual scatterers, which can be given by

$$s(t) = \sum_{k=0}^{N-1} A^{(k)} \exp(-j\frac{2\pi D^{(k)}}{\lambda}) \tag{7}$$

where t is sample time, N is the total number of raindrops positioned in a radar resolution volume, k represents different raindrops, $A^{(k)}$ represents the amplitude of the signal, $D^{(k)}$ represents the *two-way* distance (i.e. the distance from the radar to the target and back to the radar.) of the kth raindrop and represents the wavelength of the radar system. The expression of $2\pi D^{(k)}/\lambda$ represents the phase of the kth raindrop composite signal and it is worthy to note that the Doppler shift is generated by the phase of the backscattered signal from each scatterer which continuously changes with time. It is the diversity of raindrop velocities around wake vortices that results in a variety of Doppler shift frequencies. In time series, the position of each raindrop is updated based on the velocity field of rain phase and pulse repetition time (PRT) of the radar system and is approximately defined by

$$x_i^{(k)}(n+1) = x_i^{(k)}(n) + u_i^{(k)}(n) T_s \tag{8}$$

where $x_i^{(k)}(n)$ and $u_i^{(k)}(n)$ represents the position and the velocity of the kth raindrop at the nth sample time, respectively, and T_s is the PRT. The sampling interval should be small enough to ensure the accuracy of the position updating. It needs to be emphasized that the velocity $u_i(n)$ of each raindrop is derived from the interpolation based on multiphase-flow numerical simulation at all sample times. After a certain number of scatterers are inserted into the rain phase flow field, the initial velocities of the raindrops are calculated through interpolation and the volume fraction or concentration of the rain phase obtained from the numerical

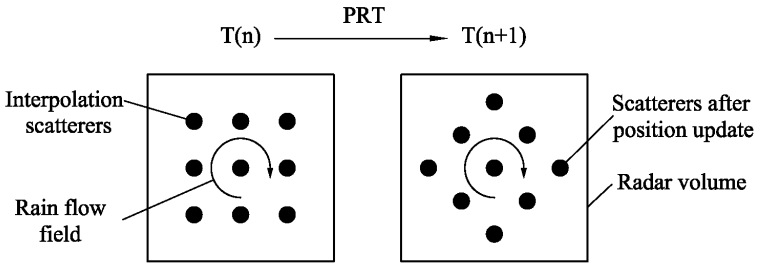

FIGURE 3. Schematic diagram of position update of scatterers with time.

simulation reflects the quantitative weighting of the raindrops in space. In this way, the new position of raindrops can be obtained through the expression (8) during the sampling interval and at the next sample time the velocities of the raindrops in these positions are interpolated again based on the numerical simulation result at the current flowtime as shown in Figure 3. By repeating this procedure, the position of raindrops can be updated for each sampling time.

B. WEIGHTING FUNCTIONS

According to the radar equation, the amplitude of the received signal, $A^{(k)}$, is defined by

$$A^{(k)} = \sqrt{\frac{P_t G^2 \lambda^2 \sigma}{(4\pi)^3 L r^4}} w_a w_r \tag{9}$$

where P_t is the transmitted peak power, G is the antenna gain, λ is the wavelength, L is the power loss, σ is the backscattering cross section of the raindrop, which calculated by Rayleigh formulas for 10 Hz X-band radar [14], [15], r is the distance of the raindrop relative to the radar and w_a, w_r represent the angular and range weighting function [6], respectively, which given by

$$w_r = \exp[\frac{(r - r_0)^2}{(0.7c\tau/2)^2}] \tag{10}$$

and

$$w_a = \exp[-\frac{(\theta - \overline{\theta})^2}{2\theta_0^2} - \frac{(\phi - \overline{\phi})^2}{2\phi_0^2}] \tag{11}$$

where r_0 represents the distance from the radar volume center to the radar, c is the speed of the light, τ is the pulse width.

V. SIMULATION AND DISCUSSION

A. THE EFFECT OF RAIN ON WAKE VORTEX DECAY

The decay of wake vortices contains two phases: the turbulent diffusion phase and fast decay phase. The former phase is in the early stage of vortex pair evolution, in which the circulation (or intensity) decays at a relatively small rate and vortex pairs are straight or became slightly deformed. In the latter phase, however, vortex pairs have obvious deformation, the circulation also decays rapidly and the straight vortices gradually develop into vortex rings. Figure 4 shows the evolution of circulation against normalized time ($t^* = t/t_0$). The circulation used in this paper is Γ_{5-15}, which is averaged over circles with radii from 5 to 15 m. The direction of vorticity integrated is perpendicular to the flight direction. Γ^*_{5-15} is a non-dimension quantity normalized by the initial circulation as follows:

$$\Gamma^*_{5-15} = \frac{1}{11} \sum_{r=5\mathrm{m}}^{15\mathrm{m}} (\int_0^r \omega \mathrm{dA}) / \Gamma_0 \tag{12}$$

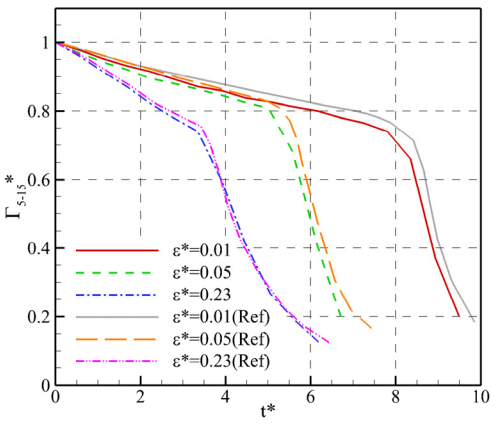

FIGURE 4. Circulation evolution for different ambient turbulence.

Figure 4 indicates that the ambient turbulent intensity has a limited impact on the rate of vortex decay in the early stage of vortex pair evolution. However, the boundary turbulence phase has a close correspondence with the intensity: the onset time of the fast decay phase decreases with increasing intensity. By comparing with Ref. [16], it can be seen that the result in this paper is in good agreement with that, which implies that the simulation of wake vortices evolution in clear air is enough accurate.

Under rainy conditions (small and medium rainfall rate) wake vortices still maintain two-phase evolution characteristics, because the very small volume fraction of raindrops is not enough to generate large momentum exchange with wake vortices. The magnitude of rain rates affects the exchange of momentum. The larger the rainfall rate or volume fraction, the greater the effective density of raindrops and the stronger the dragging effect on wake vortices. Figure 5 shows the vortex structure under different rainfall rates at $t^* = 5$ and it is represented by the iso-surface of vorticity magnitude

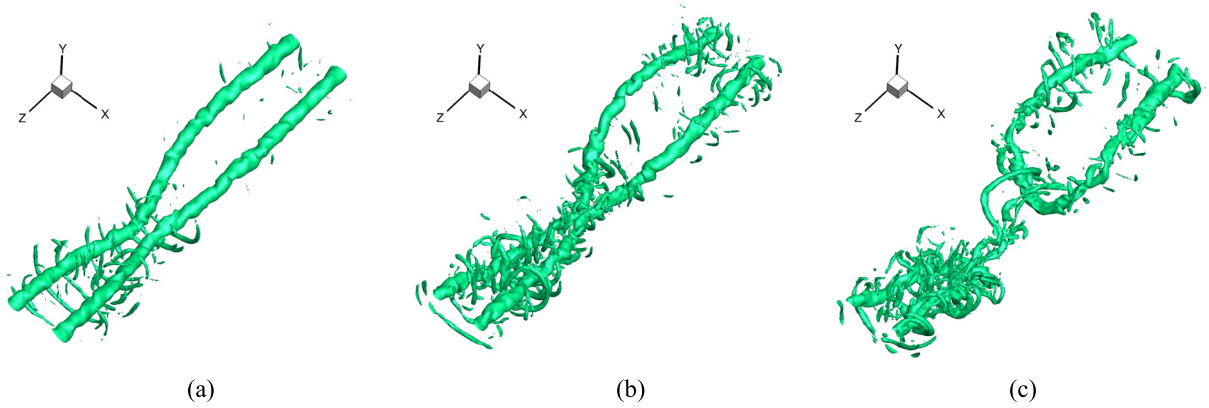

FIGURE 5. Vortex structure for varying rainfall rates with $\varepsilon^* = 0.05$ at $t^* = 5$: (a) R = 0 mm/h, (b) R = 5 mm/h and (c) R = 10 mm/h.

of 2 s^{-1}. It can be seen that wake vortices in rain have the same evolution process with that in clear air: from straight vortices to deformed vortices and then to vortex rings. Due to the effect of rainfall the deformation of wake vortices is earlier than that in clear air.

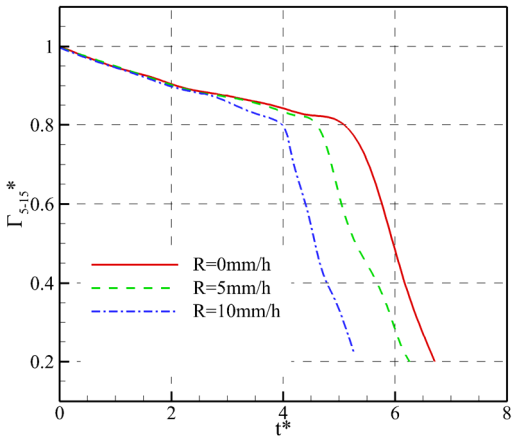

FIGURE 6. Circulation evolution for various rainfall rates.

Figure 6 shows the circulation of wake vortices under three rain rates. It is also seen that the larger the rain rate the faster the decay of wake vortices. This is because wake vortices transmit the energy to raindrops and large volume fractions transmit more energy than small ones. However, due to the volume fraction of raindrops in the air, the exchange of energy is limited and this causes that the effect of rainfall rate on wake vortex dissipation is much less than that of atmospheric turbulence.

B. CHARACTERISTICS OF RAINDROPS MOTION IN WAKE VORTEX FIELDS

Because of the tracking characteristics, the trajectory and velocity of raindrops are greatly affected by the intensity and position of wake vortices. Therefore the motion of raindrops can reflect the main characteristics of wake vortices and the response of raindrops can be further used to retrieve the circulation.

Figure 7 shows the velocity magnitude of the wake vortex and the streamline of the rain phase for the rainfall rate of 10 mm/h. The rainfall is treated as a continuous phase in this study and therefore these streamlines can be regarded as the trajectory of raindrops. As shown in Figure 7, the trajectory of raindrops is significantly affected by the wake vortex field. The trajectory has changed in shape and density and this leads to the modification of the concentration and velocity of the drops. As illustrated in Figure 7, in the presence of wake vortices, the distribution of raindrops is disturbed. It can be seen that the concentration of raindrops is reduced and enhanced by the vortex flow in different areas. Raindrop concentration decreases in the region below the vortex core due to few raindrops through this area and however in the area between the two vortex cores the concentration increases due to the vortex flow. The modified concentration will be reflected in the radar signature since the increase and decrease of concentration affect the reflectivity of the local area. Moreover, the velocity of raindrops is approximately equal to that of the vortex flow near the vortex core and this will result in the increase of Doppler width of radar signal.

C. RADAR DOPPLER SIGNATURES

To analyze radar characteristics of raindrops in wake vortices, the simulated radar echo signals are requested first. In addition to the rain-phase flow filed obtained by the numerical simulation, radar parameters and the position relationship between the radar and wake vortex are also significant for the radar signal process. In the simulation, the configuration of the side-looking radar is adopted as shown in Figure 8. YOZ is the scan plane of the radar which is set to perpendicular to the vortex axis. The antenna points in the direction of the wake vortex and the elevation will be adjusted according to the position of the wake vortex at different times. In the area near the wake vortex, the space is divided into four radar resolution volumes and the resolution range is set to 25m. The initial position of the wake vortex is placed in the two volumes

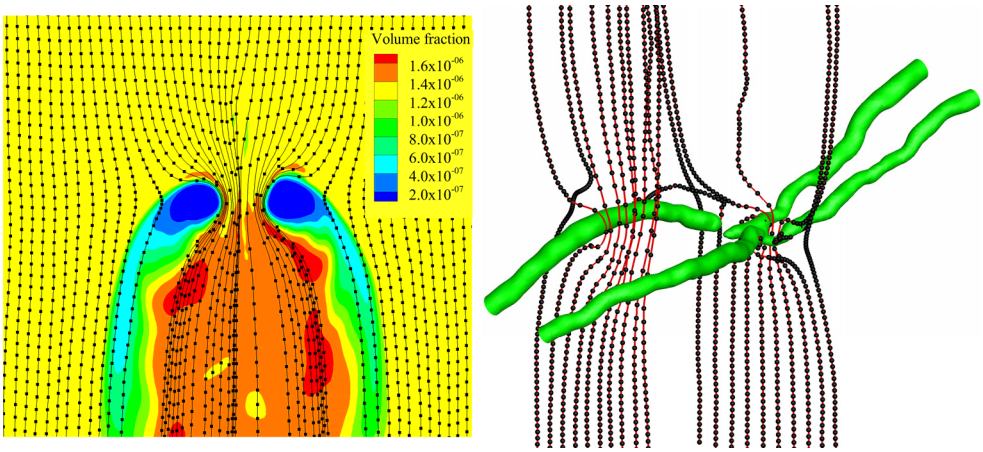

FIGURE 7. Streamline and concentration of rain phase.

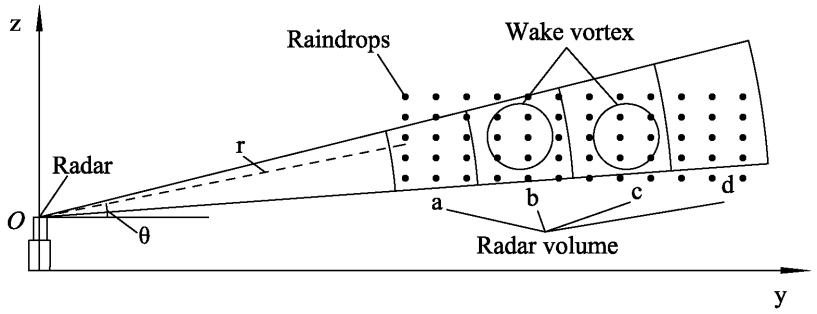

FIGURE 8. Geometric configuration of the radar simulation. R denotes the distance between the kth raindrop and the radar; θ denotes antenna beam-pointing direction angle.

TABLE 1. Input parameters of the radar simulator.

Parameter	Value
Transmitted peak power	20 W
Antenna gain	30 dB
Frequency of operation	10G HZ
Beam width	2.8°
Rain rate	5 mm/h, 10 mm/h
Distance between the radar and the aircraft	500 m
Number of samples generated	1024
Pulse repetition frequency	3348 HZ

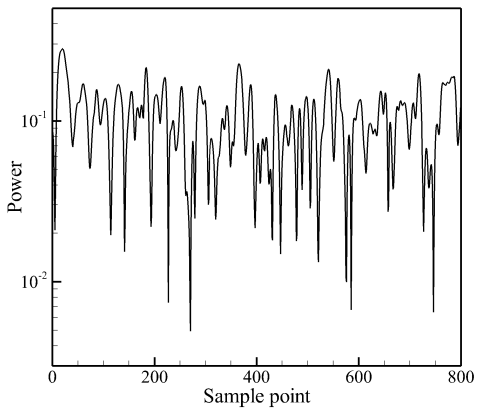

FIGURE 9. Power of the radar original signal at the straight vortex phase.

in the middle. The input parameters of the radar simulator used to generate time series of radar signals are displayed in Table 1.

As described in the previous section, rain phase is treated as a continuous medium in the simulation and therefore a certain number of discrete points are inserted into the rain phase flow field to obtain scatterers. The Doppler velocity of each raindrop is derived from the interpolation of different positions in the flow field. For a radar volume, the original radar signal is the sum of radar echo of each individual raindrop. Figure 9 shows the original echo signal of a time series in a radar volume (sample point from1 to 800). It can be seen that the obvious fluctuation of signal amplitude due to the position update of raindrops at different times.

To evaluated spectrum characteristics of radar echo signals, 256 sample points are treated with an FFT to obtain the

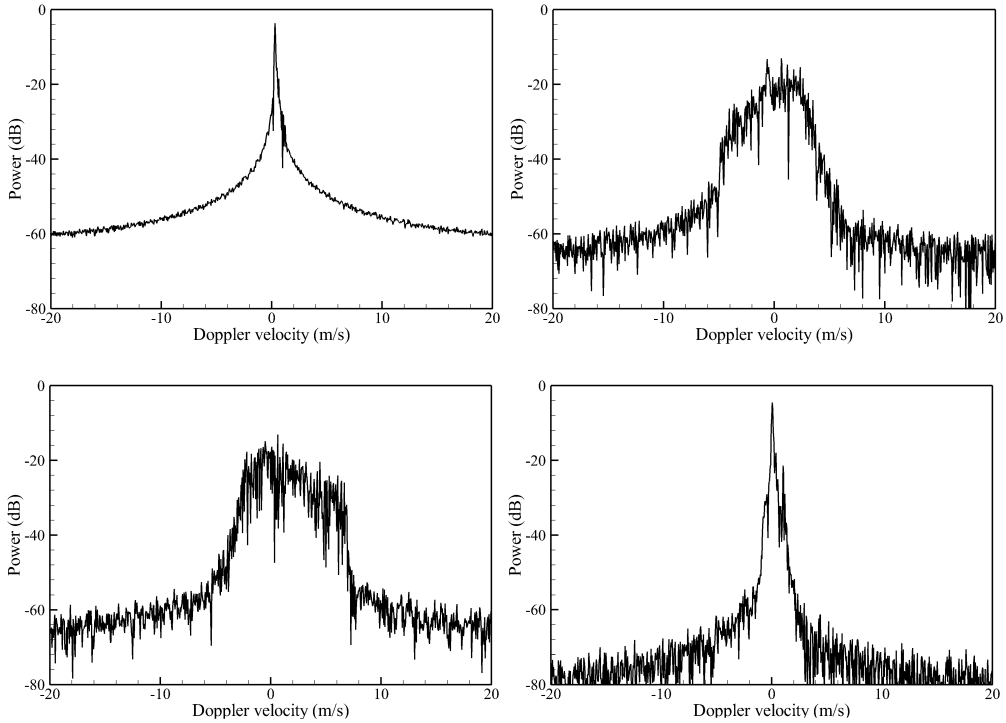

FIGURE 10. Doppler spectrum of raindrops around the straight vortex for R = 10mm/h.

complex amplitude with respect to the frequency. The various frequencies reflect the different velocities of raindrops relative to the radar in each radar resolution volume. The power carried by each frequency can be represented as the square of the mode of amplitudes. The frequency can be converted into the Doppler velocity through the relationship $v_d = \lambda f_d/2$, where v_d, λ and f_d are the Doppler velocity, the speed of light and the Doppler frequency, respectively. Actually, the Doppler spectrum expresses the power weights of raindrops with different velocities. Therefore, due to the various velocities of raindrops relative to the radar, the Doppler spectrum width around wake vortices is wider than that without wake vortices.

Due to the evolution of wake vortices, the velocity and location of raindrops are updated in time. Therefore, the Doppler frequency of raindrops within a radar volume varies with vortex decay. To investigate the relationship between the Doppler frequency of raindrops and the evolution phase of wake vortex, the Doppler spectrum of raindrops within the straight and deformed vortices are discussed. Figures 10 and 11 show the Doppler spectrum in two phases of wake vortex evolution obtained by performing FFT on 1024 sample points.

In the straight vortex phase, the two vortices are located in two adjacent radar volumes as shown in Figure 10. In Figure 10, it can be seen that the Doppler width of the radar volume b and c is wider than that of the volume a and d. The Doppler width of the volume b and c indicates the range of the Doppler velocity of raindrops is of the order of from -5m/s to 5m/s. This range agrees well with the numerical simulation results of the rain flow field and this agreement proves the radar simulator is an effective tool for simulating the radar signal. The spectrum width in the volume b and c is derived from the variety of raindrop velocities. Wake vortices drive raindrops to move in two directions relative to radar: motion toward or away from the radar corresponding to positive and negative Doppler velocities, respectively. For the volume a and d, the raindrops trend to move downward and the velocity component relative to the radar is slight and hence the spectrum width is almost zero. For a given aircraft type and its corresponding radar scan bin size, the radar signal shown in Figure 10 indicates the existence of a wake vortex and in addition, the wake vortex is in the straight vortex phase, which means that the wake vortex remains high intensity.

For the fast decay phase, lager deformation of wake vortices occurs. At certain stations the vortex pair begins to link and however the vortex separation increases at other stations. In this phase, the intensity of wake vortices decreases rapidly. Due to the change of the structure and intensity of wake vortices, the radar signal is also different from the straight vortex phase in rainy conditions. Since the vortex separation varies at the vortex axis direction, two scan positions are adopted as shown in Figure 11. It can be seen that there is Doppler width in all four radar volumes at the station with larger vortex separation, which means the wake vortex flow has entered the volume a and d. It is indicated that the vortex separation at this scanning position is increasing due to the

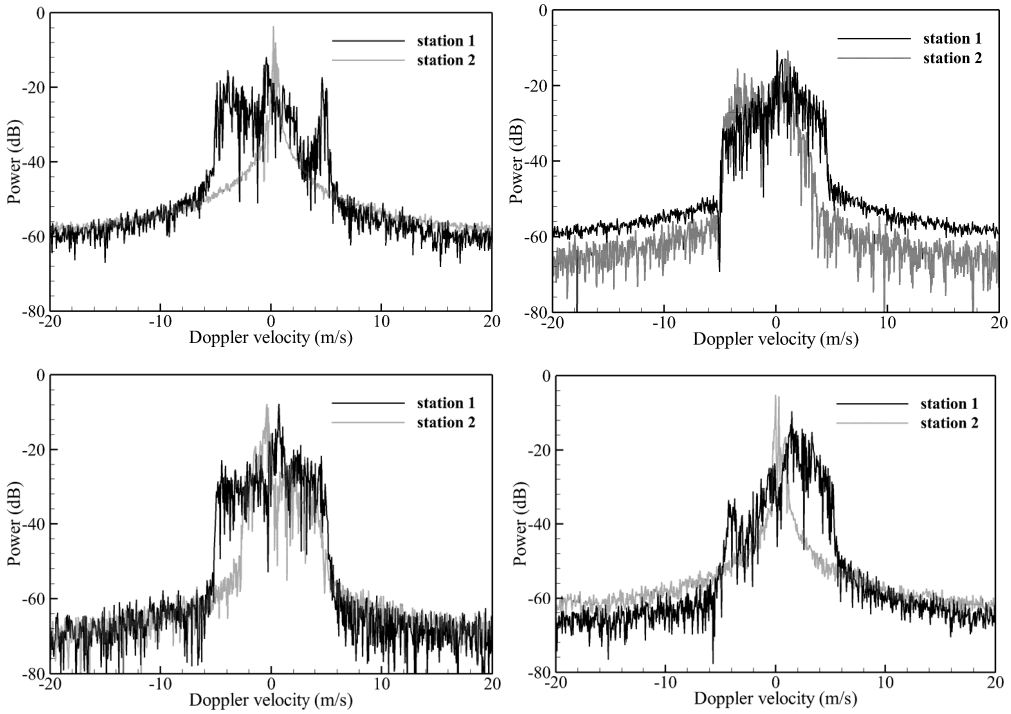

FIGURE 11. Doppler spectrum of raindrops at varying stations for fast decay phase: station 1 corresponds the position of larger vortex separation and station 2 corresponds the position of vortex linking.

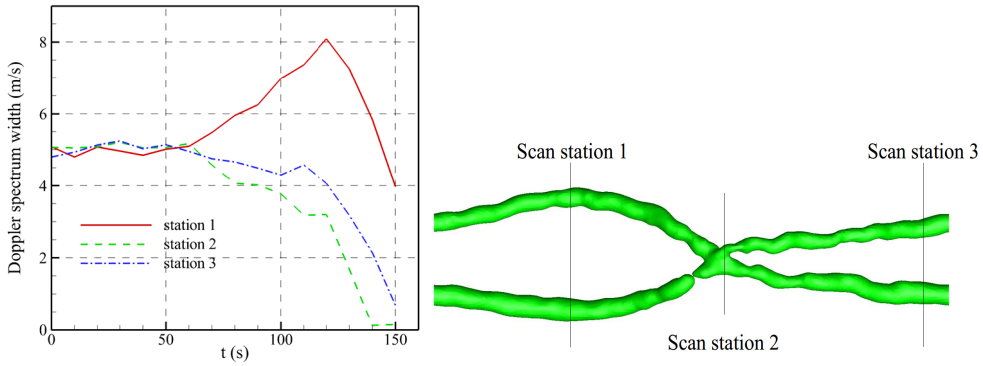

FIGURE 12. Doppler spectrum width for three different radar scan stations.

Crow instability. If the scanning range is adjusted according to the size of the vortex ring, the Doppler width of the middle volume may disappear since vortices move completely to the outermost radar volumes. When this radar signal is presented, it means that the wake vortex has entered the fast decay phase. For the case of the scanning plane at the position of the vortex linking, the Doppler spectrum is similar to that of the straight vortex as shown in Figure 11. Comparing with the Doppler spectrum of the straight vortex, the Doppler width at this position is narrower. For a vortex ring the intensity (circulation calculated parallel to the flight direction) at the position of the vortex linking is the smallest on the whole vortex axis because the approach and combination of the vortex pair occur. Hence the reduction of the Doppler width in the same radar volume also illustrates the vortex is in the fast decay phase.

To further assess the relationship between the Doppler spectrum width and the wake vortex intensity, the radar simulator is used for the whole vortex age and the results of 5 mm/h and 10mm/h are averaged to reduce the effect of uncertain rain rates. Figure 12 shows the Doppler spectrum width averaged over the four resolution volumes for three different radar scan stations. In the early stage of vortex evolution (before t = 65 s), the three stations have the same spectrum width and this is due to the stable the intensity and shape of the vortex pair. However, during the stage between t = 65 s and t = 115 s, the lines are separated from each other because of the deformation of the vortex as

discussed previously. After t = 115 s, the spectrum width of all stations rapidly decreases with the fast decay of the wake vortex and for station 2, especially, the spectrum width disappears soon that results from the formation of the vortex ring and the disconnection of vortex link.

VI. CONCLUSION

This paper has simulated the evolution of wake vortices in rainy conditions using the Eulerian-Eulerian multiphase model. LES of the wake vortex evolution have been performed and through the interphase force the momentum of the wake vortex is transmitted to the rainy phase. Comparing with the Euler–Lagrange model, the approach takes the effect of raindrops dynamics on the wake vortex evolution into account. The characteristic of the wake vortex evolution under rainy conditions and it is found that rainfall can slightly accelerate the vortices decay. The other advantage of this approach is that the initial and boundary conditions of rainfall such as the concentration and velocity can be more directly controlled.

A radar simulator has been represented for simulating radar signals of raindrops within the wake vortex. The radar parameters of X-band have been adopted to compute the radar echo signal of raindrops. Through inserting scatterer particles into the rain phase flow filed, the continuous phase is converted to discrete raindrops and the velocity and position are updated in time for generating the radar echo. The Doppler spectrum of echo signals in radar resolution volumes has been analyzed at two evolution phases of wake vortices: the straight vortex and the vortex ring. It is found that the spectrum width will appear in different radar volumes with the change of the evolution phase of wake vortices, which indicates the deformation of the vortex structure.

The Doppler spectrum analysis based on the unsteady rain phase simulation can estimate the decay stage of wake vortices, assess the vortex strength, provide data support for wake vortex monitoring under rain conditions and identify the potential hazard during the approach phase in the traffic control.

REFERENCES

[1] M. Harris, R. I. Young, F. Köpp, A. Dolfi, and J.-P. Cariou, "Wake vortex detection and monitoring," *Aerosp. Sci. Technol.*, vol. 6, no. 5, pp. 325–331, Sep. 2002.
[2] A. R. Jameson and A. B. Kostinski, "Partially coherent backscatter in radar observations of precipitation," *J. Atmos. Sci.*, vol. 67, no. 6, pp. 1928–1946, Jun. 2010.
[3] H. Sauvageot, *Radar Meteorology*. Norwood, MA, USA: Artech House, 1992.
[4] C. Capsoni and M. D'Amico, "A physically based radar simulator," *J. Atmos. Ocean. Technol.*, vol. 15, no. 2, pp. 593–598, Apr. 1998.
[5] B. L. Cheong, M. W. Hoffman, and R. D. Palmer, "Efficient atmospheric simulation for high-resolution radar imaging applications," *J. Atmos. Ocean. Technol.*, vol. 21, no. 2, pp. 374–378, Feb. 2004.
[6] B. L. Cheong, R. D. Palmer, and M. Xue, "A time series weather radar simulator based on high-resolution atmospheric models," *J. Atmos. Ocean. Technol.*, vol. 25, no. 2, pp. 230–243, Feb. 2008.
[7] Z. Liu, N. Jeannin, F. Vincent, and X. Wang, "Modeling the radar signature of raindrops in aircraft wake vortices," *J. Atmos. Ocean. Technol.*, vol. 30, no. 3, pp. 470–484, Mar. 2013.
[8] Z. Liu, N. Jeannin, F. Vincent, and X. Wang, "Development of a radar simulator for monitoring wake vortices in rainy weather," in *Proc. IEEE CIE Int. Conf. Radar*, Oct. 2011, pp. 284–287.
[9] F. Barbaresco, N. Jeannin, and V. Brion, "Radar wake-vortices cross-section/Doppler signature characterisation based on simulation and field tests trials," *IET Radar, Sonar Navigat.*, vol. 10, no. 1, pp. 82–96, Jan. 2016.
[10] J. Li, T. Wang, H. Gao, and X. Wang, "Circulation retrieval of wake vortex under rainy condition with a radar," in *Proc. IEEE Radar Conf. (RadarConf)*, May 2017, pp. 0095–0100.
[11] S. H. Huang and Q. S. Li, "Numerical simulations of wind-driven rain on building envelopes based on eulerian multiphase model," *J. Wind Eng. Ind. Aerodynamics*, vol. 98, no. 12, pp. 843–857, Dec. 2010.
[12] R. S. Rogallo, "Numerical experiments in homogeneous turbulence," NASA, Washington, DC, USA, Tech. Rep. NASA-TM-81315, 1981.
[13] W. Bechara, C. Bailly, P. Lafon, and S. M. Candel, "Stochastic approach to noise modeling for free turbulent flows," *AIAA J.*, vol. 32, no. 3, pp. 455–463, Mar. 1994.
[14] K. Shariff and A. Wray, "Analysis of the radar reflectivity of aircraft vortex wakes," *J. Fluid Mech.*, vol. 463, pp. 121–161, Jul. 2002.
[15] J. Li, X. Wang, T. Wang, and Z. Liu, "Study on the scattering characteristics of stable-stage wake vortices," in *Proc. Int. Radar Conf.*, Oct. 2009, pp. 1–5.
[16] I. Hennemann and F. Holzäpfel, "Large-eddy simulation of aircraft wake vortex deformation and topology," *Proc. Inst. Mech. Eng., G, J. Aerosp. Eng.*, vol. 225, no. 12, pp. 1336–1350, Sep. 2011.

ZHOU JIN-XIN was born in Liaoning, China, in 1987. He received the bachelor's degree in mechanical engineering from Shenyang Aerospace University, in 2009, and the master's degree in mechanical engineering from the Lanzhou University of Technology, in 2017. He is currently pursuing the Ph.D. degree with the Institute of Aviation, Northwestern Polytechnical University, Xi'an, China.

His research interests include the development of aerodynamic force and the evolution of aircraft wake vortices.

LI DONG was born in Baoji, Shaanxi, China, in 1970. He received the Ph.D. degree in aerodynamics from Northwestern Polytechnical University.

From 2002 to 2004, he held a postdoctoral position at the Department of Aeronautics and Astronautics, Nagoya University, Japan. He is currently a Professor with Northwestern Polytechnical University. He has published more than 50 articles as the first author in journals and conferences at home and abroad. His research interests include aerodynamics design and boundary layer flow control.

ZHANG ZE-YU was born in Xi'an, Shaanxi, China, in 1991. He received the bachelor's and master's degrees in mechanical engineering from the Institute of Aviation, Northwestern Polytechnical University, Xi'an, China, in 2013 and 2016, respectively, where he is currently pursuing the Ph.D. degree.

His research interests include the development of aerodynamic force and the evolution of aircraft wake vortices.